

Research Article

Research on Ambiguity Resolution Algorithm by Quaternion Based on Acoustic Vector Sensor

Guibao Wang ¹, Xinkuan Wang ¹, Lanmei Wang ², and Xiangyu Wang ¹

¹School of Physics and Telecommunication Engineering, Shaanxi University of Technology, Hanzhong 723001, China

²School of Physics and Optoelectronic Engineering, Xidian University, Xi'an 710071, China

Correspondence should be addressed to Lanmei Wang; lmwang@mail.xidian.edu.cn

Received 17 November 2019; Revised 1 September 2020; Accepted 20 October 2020; Published 20 November 2020

Academic Editor: Jesús Lozano

Copyright © 2020 Guibao Wang et al. This is an open access article distributed under the Creative Commons Attribution License, which permits unrestricted use, distribution, and reproduction in any medium, provided the original work is properly cited.

The increase in element spacing can increase the aperture of the array and improve its resolution performance. However, phase ambiguity will occur when the array element interval is larger than the minimum half wavelength of the incident signal. The three acoustic velocity components of the acoustic vector are ingeniously constructed into a new kind of quaternions because of the special structure of the acoustic vector sensor array, and the rough estimation of the direction of arrival (DOA) is obtained using the rotation relationship between the subarray steering vectors corresponding to quaternion data. The rough estimate is used to resolve the phase ambiguity of the spatial phase difference between the array elements, and the high-precision DOA estimation of the signal can be obtained. Simulation results show that the method is effective.

1. Introduction

The use of electromagnetic wave for communication or target location has become mainstream. However, the acoustic wave has more advantages than the electromagnetic wave in some special circumstances. For example, sound waves can travel around obstacles, such as mountains, rivers, and forests, and the sound source detection system can effectively detect the information of the target. The loss of acoustic wave propagation is small in water. Thus, the wave can spread for a long distance. Sonar is a key equipment in underwater communication. The acoustic vector sensor is the core part of new sonars. A single acoustic vector sensor not only can output the acoustic pressure information of the scalar sensor but also can measure the acoustic velocity information of each point directly and synchronously [1, 2]. The acoustic vector sensor consists of an acoustic pressure component sensor and a speed sensor in three-speed directions. The vibration speed sensor may be an acceleration, a displacement, or a sound pressure gradient sensor [3, 4]. In 2010, Wu et al. obtained the near-field source model of the acoustic vector

sensor by using the wave equations of the acoustic and particle velocity fields [5]. In 2012, Song et al. proposed to place the components of the three speed directions at the coordinate origin and an acoustic pressure component on one of the coordinate axes; the former is used to estimate the angle of the sound source, and the latter is used to estimate the distance information of the sound source [6]. In the array direction finding, the resolution of the angle with large array spacing will improve correspondingly. However, when the array spacing increases to more than half the wavelength of the incident signal, the pattern of the array will show grating lobes, which will lead to the ambiguity problem of parameter estimation [7, 8]. Many ways can be used to solve the ambiguity problem. Wang et al. proposed a virtual baseline method of resolving ambiguity based on the virtual ring [9]. Wong and Zoltowski proposed a uniform plane array method for solving ambiguity [10]. A nonuniform array method for solving ambiguity problems was proposed in [11], and the problem of ambiguity resolution by virtual array expansion was studied in [12]. In fact, the general mode of the ambiguity-solving method is to obtain two different

arrays through array arrangement, virtual reconstruction, or data processing. One nonsparse array without ambiguity can enable rough parameter estimation, and the other sparse array with phase ambiguity can realise accurate parameter estimation. The accurate and unambiguous estimations of the direction of arrival (DOA) are obtained by using the rough estimation of the nonsparse array to solve the phase ambiguity of the sparse array.

In recent years, array signal processing technology based on quaternion [13] has attracted increasing attention. In [14], the singular value decomposition of the quaternion matrix was studied, and a polarisation wave separation algorithm based on the real signal quaternion model was proposed. In [15, 16], the quaternion and biquaternion MUSIC algorithms for two- and three-component vector sensor arrays were proposed, respectively. In [17], the DOA estimation for the six-component electromagnetic vector sensor array was obtained using a quad-quaternion MUSIC operation. In [18], a quaternion ESPRIT algorithm based on the translation-invariant cross dipole array was proposed. These studies show that the parameter estimation algorithm based on the multivariate number has improved model error tolerance by using the constraint relationship between the different imaginary parts of the multivariate number and the strong constraint condition between the orthogonal vectors of multivariate number. In this work, a quaternion-ESPRIT algorithm for solving the direction-finding ambiguity based on the acoustic vector is proposed. This algorithm is different from the previous ambiguity-solving method. The DOA is roughly estimated using the rotation invariant relationship between the quaternion subarrays and is used to solve the phase ambiguity of the spatial steering vector. The phase ambiguity number vector is attained using the relationship between the estimated value of the phase difference between sparse elements with phase ambiguity and the rough value without ambiguity but with low accuracy. The high-accuracy estimated value without ambiguity is obtained in the end. This method has a small amount of computation and can enable high-precision DOA estimation without ambiguity.

2. Acoustic Vector Array Model

A uniform circular array is composed of M elements; R is the radius of the circular array, as shown in Figure 1. Phase ambiguity occurs when the interval between the adjacent elements is greater than the half wavelength, that is, $\Delta d > \lambda_{\min}/2$, where λ_{\min} is the minimum wavelength of the incident signal. The array elements are the acoustic vector sensors; each of these elements is composed of three orthogonal velocity sensors along the x -axis, y -axis, and z -axis, which induce the velocity component of the incoming wave signal in the x -axis, y -axis, and z -axis directions, respectively.

Assuming that K narrow-band, zero-mean, and stationary signals are incident from the far-field onto the uniform circular array shown in Figure 1, the incident direction of the k th signal source is (θ_k, ϕ_k) , $k = 1, \dots, K$, and φ_n is the angular coordinates of the n th element. The velocity compo-

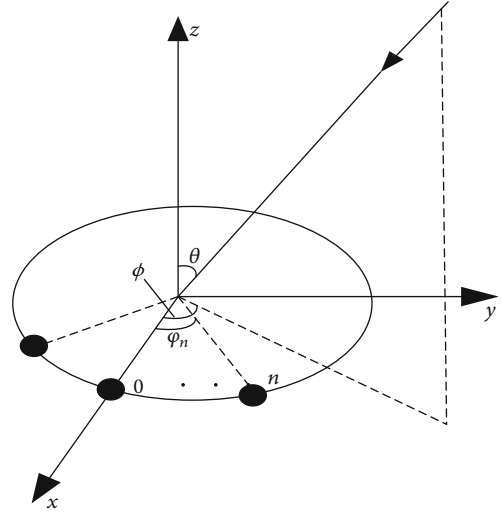


FIGURE 1: Uniform circular array geometry.

nents along the x -, y - and z -axes of the k th unit energy signal in the Cartesian coordinate system can be expressed as:

$$\mathbf{u}_k = \begin{bmatrix} v_{xk} \\ v_{yk} \\ v_{zk} \end{bmatrix} = \begin{bmatrix} \sin \theta_k \cos \phi_k \\ \sin \theta_k \sin \phi_k \\ \cos \theta_k \end{bmatrix}. \quad (1)$$

3. Quaternion Method

3.1. Mathematical Model of Quaternion Method. The x -axis velocity component v_{xk} , y -axis velocity component v_{yk} , and z -axis velocity component v_{zk} on the same array element are expressed as quaternion models as B_k :

$$\begin{aligned} B_k &= v_{zk} + i(v_{xk} + jv_{yk}) \\ &= \cos \theta_k + i(\sin \theta_k \cos \phi_k + j \sin \theta_k \sin \phi_k) \\ &= \cos \theta_k + i \sin \theta_k e^{j\phi_k} = \cos \theta_k (1 + i \tan \theta_k e^{j\phi_k}), \end{aligned} \quad (2)$$

where i and j are the imaginary parts of a quaternion.

The spatial steering vector of the array consisting of the phase difference between the M array elements and the reference origin on the circumference is as follows:

$$\mathbf{q}(\theta_k, \phi_k) = \begin{bmatrix} e^{j(2\pi R/\lambda_k) \sin \theta_k \cos(\phi_k - \varphi_1)}, \dots, e^{j(2\pi R/\lambda_k) \sin \theta_k \cos(\phi_k - \varphi_n)} \\ \dots, e^{j(2\pi R/\lambda_k) \sin \theta_k \cos(\phi_k - \varphi_M)} \end{bmatrix}. \quad (3)$$

In the formula (3) above, $\varphi_n = 2\pi(n-1)/M$, $n \in [1, \dots, M]$ represents the angular coordinates of the n th element on the circumference, and λ_k is the wavelength of the k th incident signal.

The received data of the array at t time can be expressed as:

$$\mathbf{X}_1(t) = \sum_{k=1}^K (B_k \otimes \mathbf{q}(\theta_k, \phi_k)) S_k(t) + \mathbf{N}_1(t) = \mathbf{C}_1 \mathbf{S}(t) + \mathbf{N}_1(t), \quad (4)$$

where $S_k(t)$ is the k th incident signal, \otimes represents the Kronecker product, \mathbf{C}_1 is the steering vector matrix at time t , $\mathbf{S}(t)$ is the K incident signals, and $\mathbf{N}_1(t)$ is the additive white Gaussian noise at time t .

Then, the received data of the array at $t + \Delta T$ time can be represented as:

$$\begin{aligned} \mathbf{X}_2(t) = \mathbf{X}_1(t + \Delta T) &= \sum_{k=1}^K (B_k \otimes \mathbf{q}(\theta_k, \phi_k)) e^{j2\pi f_k \Delta T} S_k(t) \\ &+ \mathbf{N}_2(t) = \mathbf{C}_2 \mathbf{S}(t) + \mathbf{N}_2(t) = \mathbf{C}_1 \Theta \mathbf{S}(t) + \mathbf{N}_2(t), \end{aligned} \quad (5)$$

where ΔT is the interval between two snapshots, f_k is the frequency of the k th signal, \mathbf{C}_2 is the steering vector matrices at time $t + \Delta T$, $\mathbf{N}_2(t)$ is the additive white Gaussian noise at time $t + \Delta T$, and

$$\Theta = \begin{bmatrix} e^{j2\pi f_1 \Delta T} & & \\ & \ddots & \\ & & e^{j2\pi f_K \Delta T} \end{bmatrix}. \quad (6)$$

So the whole received data can be written as:

$$\mathbf{Z}(t) = \begin{bmatrix} \mathbf{X}_1(t) \\ \mathbf{X}_2(t) \end{bmatrix} = \begin{bmatrix} \mathbf{C}_1 \\ \mathbf{C}_2 \end{bmatrix} \mathbf{S}(t) + \begin{bmatrix} \mathbf{N}_1(t) \\ \mathbf{N}_2(t) \end{bmatrix} = \mathbf{C} \mathbf{S}(t) + \mathbf{N}(t), \quad (7)$$

where $\mathbf{C} = \begin{bmatrix} \mathbf{C}_1 \\ \mathbf{C}_2 \end{bmatrix}$ is the whole steering vector matrix, and \mathbf{N}

$(t) = \begin{bmatrix} \mathbf{N}_1(t) \\ \mathbf{N}_2(t) \end{bmatrix}$ is the whole additive white Gaussian noise.

3.2. Quaternion Ambiguity Resolution Algorithm. The quaternion correlation matrix of the received data is \mathbf{R}

$$\mathbf{R} = E[\mathbf{Z}\mathbf{Z}^H] = \mathbf{C}E[\mathbf{S}\mathbf{S}^H]\mathbf{C}^H + E[\mathbf{N}\mathbf{N}^H] = \mathbf{C}\mathbf{R}_s\mathbf{C}^H + \sigma^2\mathbf{I}, \quad (8)$$

where $E(\cdot)$ denotes the mathematical expectation, $(\cdot)^H$ represents the conjugate transpose, $\mathbf{R}_s = E[\mathbf{S}\mathbf{S}^H]$, $E[\mathbf{N}\mathbf{N}^H] = \sigma^2\mathbf{I}$, σ^2 indicates the white noise power, and \mathbf{I} is the identity matrix.

The signal subspace \mathbf{V}_s and noise subspace \mathbf{V}_n can be obtained by quaternion eigendecomposition operations of the data correlation matrix \mathbf{R} , \mathbf{V}_1 and \mathbf{V}_2 are the first M rows and the last M rows of \mathbf{V}_s , respectively. According to the subspace theory, it can be got as follows:

$$\mathbf{V}_1 = \widehat{\mathbf{C}}_1 \mathbf{T} \quad \mathbf{V}_2 = \widehat{\mathbf{C}}_2 \mathbf{T} = \widehat{\mathbf{C}}_1 \widehat{\Theta} \mathbf{T}, \quad (9)$$

$$\mathbf{V}_1^\# \mathbf{V}_2 \mathbf{T}^{-1} = \mathbf{T}^{-1} \widehat{\Theta}, \quad (10)$$

where \mathbf{T} is the nonsingular matrix; the matrices $\widehat{\mathbf{C}}_1$, $\widehat{\mathbf{C}}_2$, and $\widehat{\Theta}$ are the respective estimates of \mathbf{C}_1 , \mathbf{C}_2 , and Θ ; $(\cdot)^\#$ denotes the pseudoinverse operator; and $(\cdot)^{-1}$ represents the inverse operation. Let $\Psi = \mathbf{V}_1^\# \mathbf{V}_2 = (\mathbf{V}_1^H \mathbf{V}_1)^{-1} \mathbf{V}_1^H \mathbf{V}_2$, then formula (10) can be expressed as:

$$\Psi \mathbf{T}^{-1} = \mathbf{T}^{-1} \widehat{\Theta}, \quad (11)$$

where the eigenvalue of Ψ constitutes the estimation $\widehat{\Theta}$ of Θ , which contains the frequency information of the source, and \mathbf{T}^{-1} is the corresponding eigenvector. The matrix factorisation of the quaternion is different from that of the long vector, that is, the eigendecomposition operation of the quaternion matrices cannot be performed directly. After the quaternion matrix is obtained, it is usually used to extract one real part and the three imaginary parts of the quaternion matrix and reconstruct the complex term to form the complex adjoint matrix. The properties of quaternion matrices are obtained by studying the properties of the plural adjoint matrix. Therefore, the corresponding information should be extracted from the quaternion matrix Ψ . Accordingly, the estimate of the steering vector \mathbf{C}_1 is obtained as follows:

$$\widehat{\mathbf{C}}_1 = \mathbf{V}_1 \widehat{\mathbf{T}}^{-1}, \quad (12)$$

where $\widehat{\mathbf{T}}^{-1}$ is the estimation of \mathbf{T}^{-1} .

3.2.1. Rough Estimate of DOA. The eigenvalue $\widehat{\Theta}$ of Ψ can be expressed as follows:

$$\widehat{\Theta} = \begin{bmatrix} e^{j2\pi \widehat{f}_1 \Delta T} & & \\ & \ddots & \\ & & e^{j2\pi \widehat{f}_K \Delta T} \end{bmatrix}, \quad (13)$$

where $\widehat{f}_1, \dots, \widehat{f}_K$ are the frequencies of the corresponding signals.

The frequency of the k th signal source can be estimated as follows:

$$\widehat{f}_k = \frac{\arg(\widehat{\Theta}_{kk})}{2\pi \Delta T}, \quad (14)$$

where $\arg(\cdot)$ denotes the operation of the extracting phase and $\widehat{\Theta}_{kk}$ is the k th row and k th column element of the matrix $\widehat{\Theta}$.

According to formulas (2) and (12), the steering vector $\widehat{\mathbf{C}}_1$ can be written as another form:

$$\widehat{\mathbf{C}}_1 = \widehat{\mathbf{C}}_{1x} + i\widehat{\mathbf{C}}_{1y}. \quad (15)$$

Among them, $\widehat{\mathbf{C}}_{1x}$ and $\widehat{\mathbf{C}}_{1y}$ satisfy the following relationships:

$$\begin{aligned}\widehat{\mathbf{C}}_{1x} &= \widehat{\mathbf{C}}_{1y} \widehat{\boldsymbol{\Phi}}_1, \\ \widehat{\boldsymbol{\Phi}}_1 &= [\widehat{\mathbf{C}}_{1y}]^\# \widehat{\mathbf{C}}_{1x} = \left(\widehat{\mathbf{C}}_{1y}^H \widehat{\mathbf{C}}_{1y} \right)^{-1} \widehat{\mathbf{C}}_{1y}^H \widehat{\mathbf{C}}_{1x},\end{aligned}\quad (16)$$

where

$$\widehat{\boldsymbol{\Phi}}_1 = \begin{bmatrix} \tan \widehat{\theta}_1 e^{j\phi_{\Lambda_1}} & & \\ & \ddots & \\ & & \tan \widehat{\theta}_K e^{j\phi_{\Lambda_K}} \end{bmatrix}. \quad (17)$$

According to formula (17), the rough estimate of DOA without ambiguity is obtained.

$$\widehat{\theta}_k = \tan^{-1} \left(|\widehat{\boldsymbol{\Phi}}_{1kk}| \right) \quad \widehat{\phi}_k = \arg \left(\widehat{\boldsymbol{\Phi}}_{1kk} \right), \quad (18)$$

where $\widehat{\boldsymbol{\Phi}}_{1kk}$ is the k th row and k th column element of the matrix $\widehat{\boldsymbol{\Phi}}_1$.

3.2.2. Ambiguity Resolution Algorithm. According to the unambiguous rough estimate of $\widehat{\theta}_k$ and $\widehat{\phi}_k$, the rough phase difference estimation $\widehat{\boldsymbol{\Omega}}_1$ can be obtained:

$$\widehat{\boldsymbol{\Omega}}_1 = \Delta \mathbf{W} \cdot \begin{bmatrix} \widehat{\Gamma}_{1k} \\ \widehat{\Gamma}_{2k} \end{bmatrix} = [\mathbf{W}_2 - \mathbf{W}_1] \cdot \begin{bmatrix} \widehat{\Gamma}_{1k} \\ \widehat{\Gamma}_{2k} \end{bmatrix}, \quad (19)$$

where $\Delta \mathbf{W} = \mathbf{W}_2 - \mathbf{W}_1$, $\mathbf{W}_1 = \mathbf{W}(1 : M - 1, :)$, $\mathbf{W}_2 = \mathbf{W}(2 : M, :)$, $\widehat{\Gamma}_{1k} = \sin \widehat{\theta}_k \sin \widehat{\phi}_k$, $\widehat{\Gamma}_{2k} = \sin \widehat{\theta}_k \cos \widehat{\phi}_k$, $\mathbf{W}(1 : M - 1, :)$ represents the submatrix extracted from the first row to M row of \mathbf{W} , and $\mathbf{W}(2 : M, :)$ represents the submatrix extracted from the second row to M row of \mathbf{W} , with

$$\mathbf{W} = (2\pi R / \lambda_k) \begin{bmatrix} \sin \varphi_1 & \cos \varphi_1 \\ \vdots & \vdots \\ \sin \varphi_M & \cos \varphi_M \end{bmatrix}. \quad (20)$$

Let

$$\widehat{\mathbf{g}}_{1k} = \widehat{\mathbf{C}}_1(1 : M - 1, k), \quad \widehat{\mathbf{g}}_{2k} = \widehat{\mathbf{C}}_1(2 : M, k), \quad (21)$$

where $\widehat{\mathbf{C}}_1(1 : M - 1, k)$ and $\widehat{\mathbf{C}}_1(2 : M, k)$ denote vectors composed of elements from row 1 to row M and from row 2 to row M in the column k of the matrix $\widehat{\mathbf{C}}_1$, respectively.

From formula (21), the estimate of spatial steering vectors $\Delta \widehat{\mathbf{q}}_k$ can be written as:

$$\Delta \widehat{\mathbf{q}}_k = [\widehat{\mathbf{g}}_{2k} \cdot / \widehat{\mathbf{g}}_{1k}], \quad (22)$$

where $[\cdot / \cdot]$ denotes the dot division which is the division corresponding elements of two vectors.

By taking the phase on both sides of equation (22), the estimated value containing the ambiguous phase difference can be expressed as:

$$\widehat{\boldsymbol{\Omega}}_2 = \arg [\Delta \widehat{\mathbf{q}}_k]. \quad (23)$$

The ambiguous vector \mathbf{P}_{omp} can be solved by the following formula:

$$\mathbf{P}_{omp} = \arg \min_{\mathbf{P}} \left\{ \left| \widehat{\boldsymbol{\Omega}}_2 + 2\pi \mathbf{P} - \widehat{\boldsymbol{\Omega}}_1 \right| \right\} \quad (24)$$

The expression $\arg \min(\cdot)$ represents the vector composed of the smallest integer satisfying the condition and \mathbf{P} is the possible vector of ambiguity numbers.

By substituting the obtained ambiguous vector into formula (25), the accurate unambiguous phase difference $\widehat{\boldsymbol{\Omega}}_3$ can be obtained as follows:

$$\widehat{\boldsymbol{\Omega}}_3 = \left[\widehat{\boldsymbol{\Omega}}_2 + 2\pi \mathbf{P}_{omp} \right] = \Delta \mathbf{W} \cdot \begin{bmatrix} \widehat{\Gamma}'_{1k} \\ \widehat{\Gamma}'_{2k} \end{bmatrix}. \quad (25)$$

From (25), the accurate DOA estimate without ambiguity is estimated as follows:

$$\begin{cases} \widehat{\theta}'_k = \arcsin \left(\sqrt{\widehat{\Gamma}'_{1k}{}^2 + \widehat{\Gamma}'_{2k}{}^2} \right), \\ \widehat{\phi}'_k = \arctan \left(\frac{\widehat{\Gamma}'_{1k}}{\widehat{\Gamma}'_{2k}} \right), \quad \widehat{\Gamma}'_{2k} \geq 0, \\ \widehat{\phi}'_k = \pi + \arctan \left(\frac{\widehat{\Gamma}'_{1k}}{\widehat{\Gamma}'_{2k}} \right), \quad \widehat{\Gamma}'_{2k} < 0. \end{cases} \quad (26)$$

4. Long Vector Method

4.1. Mathematical Model of the Long Vector Method. The received data of the acoustic velocity subarray in the x -axis, y -axis, and z -axis directions can be expressed as:

$$\begin{aligned}\mathbf{X}_x(t) &= \mathbf{A}_x \mathbf{S}(t) + \mathbf{N}_x(t), \\ \mathbf{X}_y(t) &= \mathbf{A}_y \mathbf{S}(t) + \mathbf{N}_y(t), \\ \mathbf{X}_z(t) &= \mathbf{A}_z \mathbf{S}(t) + \mathbf{N}_z(t),\end{aligned}\quad (27)$$

where $\mathbf{S}(t)$ is the incident signal; $\mathbf{N}_x(t)$, $\mathbf{N}_y(t)$, and $\mathbf{N}_z(t)$ are, respectively, the additive white Gaussian noise along the x -axis, y -axis, and z -axis directions; and \mathbf{A}_x , \mathbf{A}_y , and \mathbf{A}_z are the subarray steering vector along the x -axis, y -axis, and z -axis directions.

\mathbf{A}_x , \mathbf{A}_y , and \mathbf{A}_z can be further expressed as follows:

$$\begin{aligned}\mathbf{A}_x &= [\mathbf{a}_x(\theta_1, \phi_1), \dots, \mathbf{a}_x(\theta_k, \phi_k), \dots, \mathbf{a}_x(\theta_K, \phi_K)], \\ \mathbf{A}_y &= [\mathbf{a}_y(\theta_1, \phi_1), \dots, \mathbf{a}_y(\theta_k, \phi_k), \dots, \mathbf{a}_y(\theta_K, \phi_K)], \\ \mathbf{A}_z &= [\mathbf{a}_z(\theta_1, \phi_1), \dots, \mathbf{a}_z(\theta_k, \phi_k), \dots, \mathbf{a}_z(\theta_K, \phi_K)],\end{aligned}\quad (28)$$

where $\mathbf{a}_x(\theta_k, \phi_k) = v_{xk} \mathbf{q}(\theta_k, \phi_k)$, $\mathbf{a}_y(\theta_k, \phi_k) = v_{yk} \mathbf{q}(\theta_k, \phi_k)$, and $\mathbf{a}_z(\theta_k, \phi_k) = v_{zk} \mathbf{q}(\theta_k, \phi_k)$, with $\mathbf{q}(\theta_k, \phi_k)$ the spatial steering vector of the array; its expression is the same as formula (3).

The relationship between the three subarray steering vectors is:

$$\begin{aligned} \mathbf{A}_x &= \mathbf{A}_z \Phi_x, \\ \mathbf{A}_y &= \mathbf{A}_z \Phi_y, \end{aligned} \quad (29)$$

where

$$\begin{aligned} \Phi_x &= \begin{bmatrix} \tan \theta_1 \cos \phi_1 & & & & \\ & \ddots & & & \\ & & \tan \theta_k \cos \phi_k & & \\ & & & \ddots & \\ & & & & \tan \theta_K \cos \phi_K \end{bmatrix} \\ \Phi_y &= \begin{bmatrix} \tan \theta_1 \sin \phi_1 & & & & \\ & \ddots & & & \\ & & \tan \theta_k \sin \phi_k & & \\ & & & \ddots & \\ & & & & \tan \theta_K \sin \phi_K \end{bmatrix}. \end{aligned} \quad (30)$$

The received data of the acoustic velocity subarray along the x -axis, y -axis, and z -axis directions are arranged in sequence to form a long vector; then, the received data of the array at t and $t + \Delta T$ time can be expressed as:

$$\begin{aligned} \bar{\mathbf{X}}_1(t) &= \sum_{k=1}^K (\mathbf{u}_k \otimes \mathbf{q}(\theta_k, \phi_k)) S_k(t) + \mathbf{N}_1(t) = \bar{\mathbf{C}}_1 S(t) + \mathbf{N}_1(t), \\ \bar{\mathbf{X}}_2(t) &= \bar{\mathbf{X}}_1(t + \Delta T) = \sum_{k=1}^K (\mathbf{u}_k \otimes \mathbf{q}(\theta_k, \phi_k)) e^{i2\pi f_k \Delta T} S_k(t) \\ &+ \mathbf{N}_2(t) = \bar{\mathbf{C}}_1 \Theta S(t) + \mathbf{N}_2(t) = \bar{\mathbf{C}}_2 S(t) + \mathbf{N}_2(t), \end{aligned} \quad (31)$$

where $\bar{\mathbf{C}}_1 = [\mathbf{A}_x; \mathbf{A}_y; \mathbf{A}_z]$ is an array steering vector at time t , \otimes denotes the Kronecker product, $S_k(t)$ is the k th element of $S(t)$, $\mathbf{N}_1(t)$ is the receiving noise of the whole array at time t , $\mathbf{N}_2(t)$ is the receiving noise of the whole array at time $t + \Delta T$, $\mathbf{N}_x(t)$ is the noise received by the x -axis vibration velocity subarray, $\mathbf{N}_y(t)$ and $\mathbf{N}_z(t)$ are the noises received by the y -axis and z -axis vibration velocity subarrays, respectively, and the expression of \mathbf{u}_k is the same as formula (1). $\bar{\mathbf{C}}_2 = \bar{\mathbf{C}}_1 \Theta$ is an array steering vector at time $t + \Delta T$.

In summary, the whole received data can be written as:

$$\bar{\mathbf{Z}}(t) = \begin{bmatrix} \bar{\mathbf{X}}_1(t) \\ \bar{\mathbf{X}}_2(t) \end{bmatrix} = \begin{bmatrix} \bar{\mathbf{C}}_1 \\ \bar{\mathbf{C}}_2 \end{bmatrix} S(t) + \begin{bmatrix} \mathbf{N}_1(t) \\ \mathbf{N}_2(t) \end{bmatrix} = \bar{\mathbf{C}} S(t) + \bar{\mathbf{N}}(t), \quad (32)$$

$$\text{where } \bar{\mathbf{C}} = \begin{bmatrix} \bar{\mathbf{C}}_1 \\ \bar{\mathbf{C}}_2 \end{bmatrix}, \bar{\mathbf{N}}(t) = \begin{bmatrix} \mathbf{N}_1(t) \\ \mathbf{N}_2(t) \end{bmatrix}.$$

4.2. Long Vector Ambiguity Resolution Algorithm. The plural received data correlation matrix is:

$$\bar{\mathbf{R}} = E[\bar{\mathbf{Z}}\bar{\mathbf{Z}}^H] = \bar{\mathbf{C}}E[\mathbf{S}\mathbf{S}^H]\bar{\mathbf{C}}^H + E[\bar{\mathbf{N}}\bar{\mathbf{N}}^H] = \bar{\mathbf{C}}\mathbf{R}_s\bar{\mathbf{C}}^H + \sigma^2\mathbf{I}. \quad (33)$$

The signal and noise subspace \mathbf{U}_s and \mathbf{U}_n can be obtained by the complex domain eigendecomposition of the data correlation matrix $\bar{\mathbf{R}}$. The signal subspace is divided into front and back halves, and the estimation of signal frequency f_k and steering vector $\hat{\mathbf{C}}_1$ can be obtained by the ESPRIT method. The process is similar to Section 3.2.

where

$$\hat{\mathbf{C}}_1 = \begin{bmatrix} \hat{\mathbf{A}}_x \\ \hat{\mathbf{A}}_y \\ \hat{\mathbf{A}}_z \end{bmatrix}. \quad (34)$$

4.2.1. Rough Estimate of DOA. According to formulas (29) and (34), the following estimates can be obtained:

$$\begin{aligned} \hat{\Phi}_x &= \hat{\mathbf{A}}_z^{\#} \hat{\mathbf{A}}_x, \\ \hat{\Phi}_y &= \hat{\mathbf{A}}_z^{\#} \hat{\mathbf{A}}_y. \end{aligned} \quad (35)$$

The rough estimate value of DOA without ambiguity is given by:

$$\begin{aligned} \tilde{\theta}_k &= \tan^{-1} \left(\sqrt{\hat{\Phi}_x^2(k, k) + \hat{\Phi}_y^2(k, k)} \right), \\ \tilde{\phi}_k &= \begin{cases} \tan^{-1} \left(\frac{\hat{\Phi}_y(k, k)}{\hat{\Phi}_x(k, k)} \right) & \hat{\Phi}_y(k, k) \geq 0 \\ \pi + \tan^{-1} \left(\frac{\hat{\Phi}_y(k, k)}{\hat{\Phi}_x(k, k)} \right) & \hat{\Phi}_y(k, k) < 0 \end{cases}, \end{aligned} \quad (36)$$

where $\hat{\Phi}_x(k, k)$ and $\hat{\Phi}_y(k, k)$ are the k th row and k th column element of $\hat{\Phi}_x$. The ambiguity resolution algorithm is the same as in Section 3.2.2.

5. Performance Analysis of the Algorithm

5.1. Scope of Application Analysis. The quaternion ESPRIT parameter estimation method is convenient for estimating the roughly estimated angle of arrival of the signal. It ingeniously combines three velocity sensor subarrays into a quaternion subarray by using the rotation relationship between the quaternion subarrays. Comparing formulas (18) and (36) reveals that the quaternion method has evident advantages in calculating the rough estimation of the angle of arrival. The rotation invariant relationship between direct and delayed

sampling data can be used to estimate the parameters for narrow-band far-field signals with different frequencies; in this scenario, no requirement is imposed for the array configuration. The translation invariant relationship between subarrays should be used for parameter estimation of the same-frequency signal; this approach is only suitable for uniform array and results in array aperture loss. For uniform L-array, the eigendecomposition should be performed using the translation-invariant relationship in the x - and y -axis directions to obtain the spatial steering vector in these directions.

5.2. Computational Complexity Analysis. The following is a comparison of the computational cost of the algorithms based on the two models. Given that the amount of algorithmic computation depends on hardware and software, we only focus on the computational complexity of the covariance matrix of the algorithm. Without loss of generality, an array of M acoustic velocity vector sensors is considered. In data processing, N snapshots are used to estimate the data covariance matrix. The data covariance matrices based on the quaternion and plural model are expressed as follows:

$$\begin{aligned} \mathbf{R}_S &= \frac{1}{N} \sum_{n=1}^N \mathbf{Z}_{sn} \mathbf{Z}_{sn}^H = \frac{1}{N} \sum_{n=1}^M \mathbf{R}_{sn}, \\ \mathbf{R}_L &= \frac{1}{N} \sum_{n=1}^N \mathbf{Z}_{Ln} \mathbf{Z}_{Ln}^H = \frac{1}{N} \sum_{n=1}^N \mathbf{R}_{Ln}. \end{aligned} \quad (37)$$

Each of the array elements is composed of three orthogonal velocity sensors along the x -, y -, and z -axis directions. Quaternion is $\mathbf{Z}_{sn} \in H^M$, \mathbf{R}_{sn} contains M^2 quaternion elements, storage matrix \mathbf{R}_{sn} requires $4M^2$ machine memory units, and the multiplication of two quaternions is equivalent to 16 real multiplications and 12 real additions. The operation of the matrix \mathbf{R}_{sn} requires $16M^2$ real multiplications and 12 M^2 real additions. Thus, $16M^2N$ real multiplications, $4M^2$ real divisions, and $12M^2N + (N-1)4M^2 = 16M^2N - 4M^2$ real additions are required for the operation of the matrix \mathbf{R}_S . The plural is $\mathbf{Z}_{Ln} \in C^M$, \mathbf{R}_{Ln} contains $9M^2$ complex units, storage matrix \mathbf{R}_{Ln} requires $9M^2$ machine memory units, and the multiplication of two plurals is equivalent to 4 real multiplications and 2 real additions. The operation of the matrix \mathbf{R}_{Ln} requires $36M^2$ real multiplications and $18M^2$ real additions. Thus, the operation of the matrix \mathbf{R}_L requires $36M^2N$ real multiplications, $18M^2$ real divisions, and $18M^2N + (N-1)9M^2 = 27M^2N - 9M^2$ real additions. Under the same array conditions, the storage units needed for the calculation of the quaternion covariance matrix and the real number addition, multiplication, and division operations are less than those for the long-vector method.

6. Simulation Experiment and Analysis

The proposed algorithm in this paper is applicable to uniform linear array, uniform circular array, and so on. Without loss of generality, the simulation experiment takes uniform circular array as an example. Two far-field, narrow-band, non-Gaussian stationary sound signals are inci-

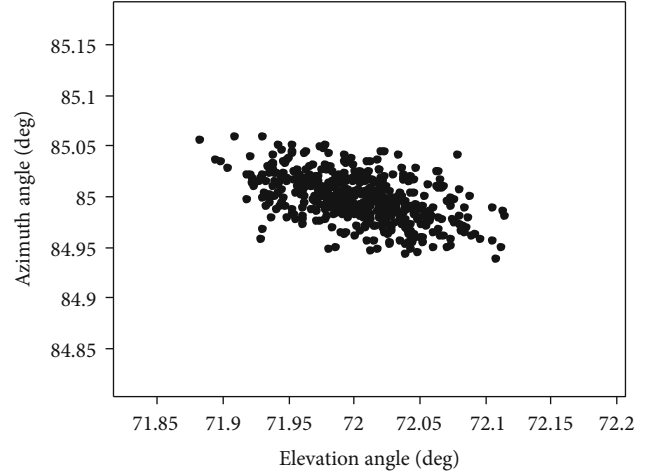


FIGURE 2: DOA scatter diagram using the quaternion method.

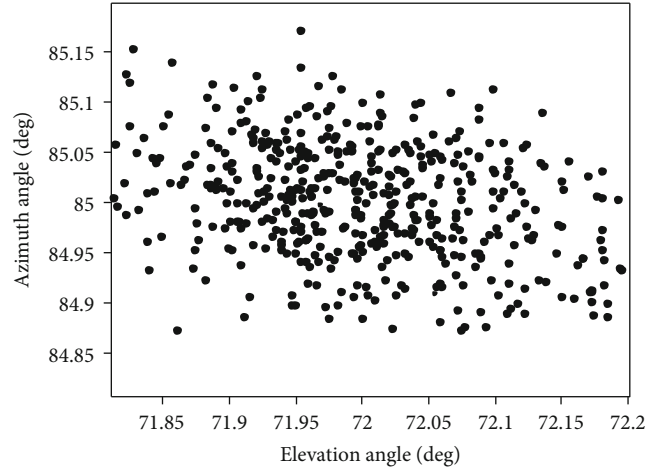


FIGURE 3: DOA scatter diagram using the long vector method.

dent into the uniform circular acoustic vector sensor array shown in Figure 1. The receiving array is composed of 9 array elements; the incident signal parameters are set as follows: $(\theta_1, \phi_1) = (72^\circ, 85^\circ)$, $(\theta_2, \phi_2) = (30^\circ, 40^\circ)$, digital frequencies $(f'_1, f'_2) = (0.75, 0.45)$, the interelement d with ambiguity is $2.5\lambda_{\min}$, 200 Monte Carlo experiments, and the noise is zero-mean additive white Gaussian noise.

6.1. Simulation Experiment. Figures 2 and 3 are the scatter diagrams of the estimated results, the number of snapshots is 50, and the SNR is set to 20 dB. From the intuitive comparison of the two graphs, it can be seen that the elevation and azimuth angles of the quaternion deambiguity algorithm are more concentrated around the actual value, while the angle estimation of the long vector deambiguity algorithm is more scattered. It is shown that the quaternion deambiguity algorithm has a little improvement in parameter estimation accuracy compared with the long vector deambiguity algorithm, but the calculation amount and storage space of the quaternion deambiguity algorithm is much less than that of the long vector deambiguity algorithm.

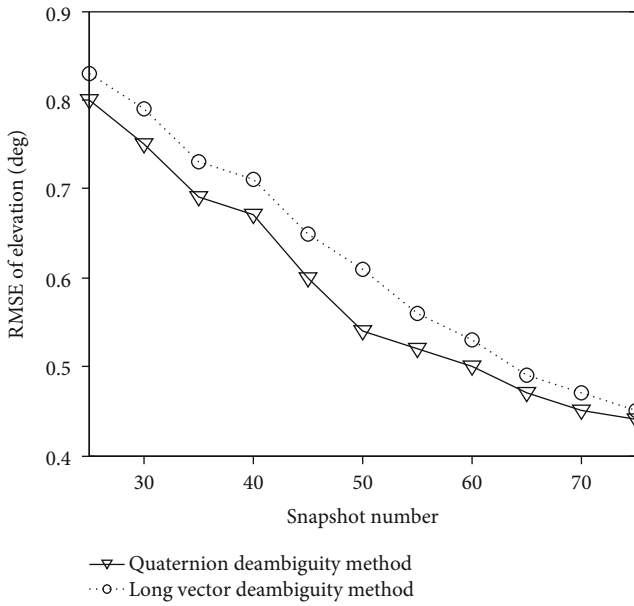


FIGURE 4: The RMSE of elevation versus the snapshot number.

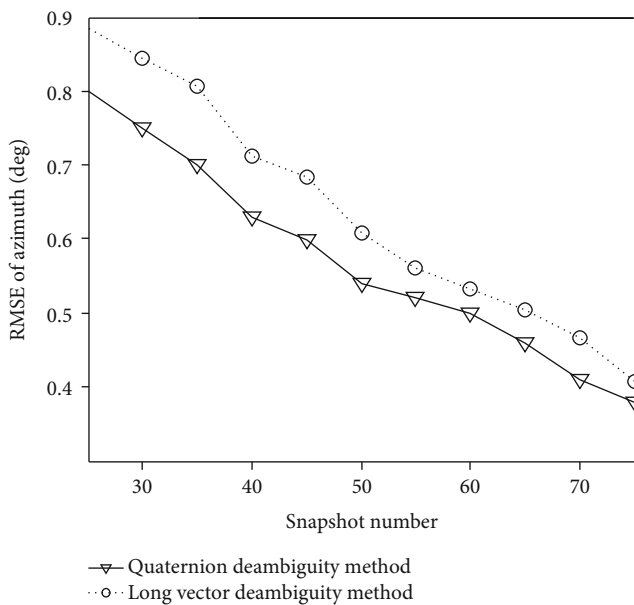


FIGURE 5: The RMSE of azimuth versus the snapshot number.

Figures 4 and 5 plot the root mean square error (RMSE) of elevation angle and azimuth angle, respectively estimated by long vector and quaternion de-ambiguity method, at different snapshot number levels. The SNR is set as 10 dB. It can be seen from Figures 4 and 5 that the RMSE of the elevation and azimuth angles of the two algorithms decreases with the increase of the number of snapshots. The RMSE performance of the quaternion-based de-ambiguity algorithm is better than that of the long vector de-ambiguity algorithm in the snapshot number range from 25 to 75.

Figures 6 and 7 show the success probability of the elevation angle and azimuth angle, respectively, estimated by the

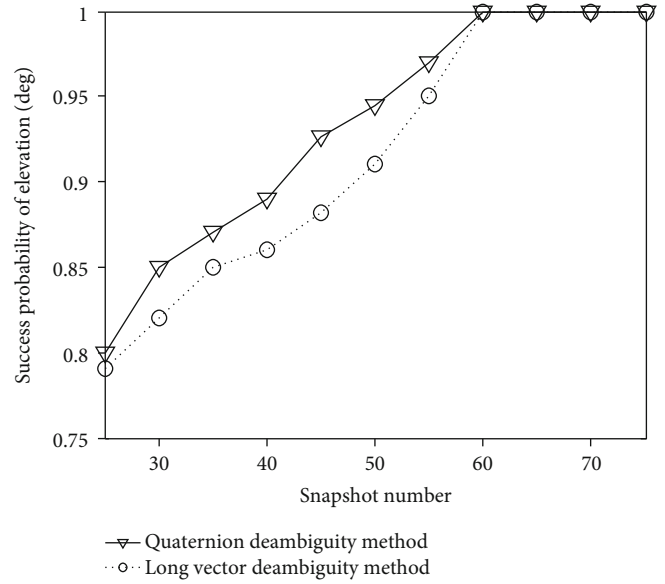


FIGURE 6: The success probability of elevation.

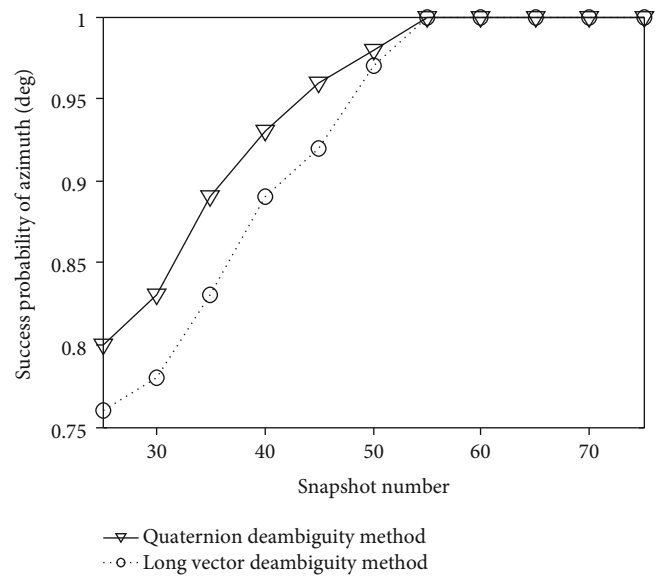


FIGURE 7: The success probability of azimuth.

long vector and quaternion de-ambiguity method, at different snapshot number levels. The SNR is set as 10 dB. It can be seen that the success probability of elevation and azimuth angles of the two algorithms increase with the increase of the number of snapshots. The success probability of the elevation angle and azimuth angle based on the quaternion-based de-ambiguity algorithm is better than that of the long vector de-ambiguity algorithm in the snapshot number range from 25 to 60 and from 25 to 55, respectively.

6.2. Performance Analysis. The proposed method needs a quaternion eigendecomposition and a complex eigendecomposition. The eigenvalue of the plural eigendecomposition can be used to calculate the rough estimate of the direction of arrival of the signal, and the eigenvectors constitute the estimation of

the spatial steering vector. The parameters are automatically paired, and no additional pairing operations are required. However, the long-vector method needs to divide the signal subspace into three subarrays corresponding to the steering vectors along the x , y , and z -axes. The complex eigendecomposition of the full data must be performed, and two additional complex eigendecompositions are needed. The eigenvectors of the two latter eigendecompositions are used to estimate the steering vector and the direction of arrival of the signal. The two eigendecompositions are performed separately, and additional pairing operations are required.

7. Conclusion

The proposed phase ambiguity resolution method of the sparse array can effectively improve the estimation accuracy of parameters and the flexibility of array placement. A set of rough and unambiguous estimates of DOA can be given very conveniently through the ingenious combination of three acoustic velocity sensors into quaternion data. Thus, the phase ambiguity of the sparse array steering vector can be solved, and high-precision DOA estimates are herein obtained. The vector orthogonality between the quaternion data components is fully utilised, and the automatic matching of the eigenvalues and eigenvectors does not require additional matching operations. The quaternion method is less computationally complex than the long-vector method. ESPRIT of the long vector can be applied to arbitrarily distributed arrays in space and has a wide application range.

Data Availability

All data included in this study are available upon request by contact with the corresponding author.

Conflicts of Interest

The author(s) declare(s) that they have no conflicts of interest.

Acknowledgments

This work was supported by the National Natural Science Foundation of China under contract (61772398, 61972239), the Key Research and Development Program Projects of Shaanxi Province (2019SF-257, 2020GY-024), the Opening Foundation of Shaanxi University of Technology Shaanxi Key Laboratory of industrial Automation (SLGPT2019KF01-15), and the Science and Technology Program of Hantai District (2019KX-21). The authors would like to thank the anonymous reviewers and the associated editor for their valuable comments and suggestions that improved the clarity of this manuscript.

References

[1] A. Agarwal, A. Kumar, M. Aggarwal, and R. Bahl, "Design and experimentation with acoustic vector sensors," in *IEEE Proceedings of SYMPOL*, pp. 139–146, 2009.

[2] X. Yuan, "Direction-finding with a misoriented acoustic vector sensor," *IEEE Transactions on Aerospace and Electronic Systems*, vol. 4, no. 2, pp. 1809–1815, 2012.

[3] M. K. Awad and K. T. Wong, "Recursive least-squares source tracking using one acoustic vector sensor," *IEEE Transactions on Aerospace and Electronic Systems*, vol. 48, no. 4, pp. 3073–3083, 2012.

[4] X. Yuan, "Coherent source direction-finding using a sparsely-distributed acoustic vector-sensor array," *IEEE Transactions on Aerospace and Electronic Systems*, vol. 48, no. 3, pp. 2710–2715, 2012.

[5] Y. I. Wu, K. T. Wong, and S. K. Lau, "The acoustic vector-sensor's near-field array-manifold," *IEEE Transactions on Signal Processing*, vol. 58, no. 7, pp. 3946–3951, 2010.

[6] Y. Song and K. T. Wong, "Closed-form direction finding using collocated but orthogonally oriented higher order acoustic sensors," *IEEE Sensors Journal*, vol. 12, no. 8, pp. 2604–2608, 2012.

[7] L. M. Wang, L. Yang, G. B. Wang, and S. Z. Wang, "DOA and polarization estimation based on sparse COLD array," *Wireless Personal Communications*, vol. 85, no. 4, pp. 2447–2462, 2015.

[8] J. Z. Liu, Z. Q. Zhao, Z. Y. He, and Z. P. Nie, "Resolving manifold ambiguities for direction-of-arrival estimation of sparse array using semi-circular substrates," *IET Microwaves Antennas & Propagation*, vol. 7, no. 12, pp. 1016–1020, 2013.

[9] L. M. Wang, J. P. Lin, G. B. Wang, and Z. H. Chen, "A direction finding technique using millimeter-wave interferometer," *Journal of Infrared and Millimeter Waves*, vol. 34, no. 2, pp. 140–144, 2015.

[10] K. T. Wong and M. D. Zoltowski, "Direction-finding with sparse rectangular dual-size spatial invariance array," *IEEE Transactions on Aerospace and Electronic Systems*, vol. 34, no. 4, pp. 1320–1336, 1998.

[11] L. M. Wang, G. B. Wang, and Z. H. Chen, "Joint DOA-polarization estimation based on uniform concentric circular array," *Journal of Electromagnetic Waves and Applications*, vol. 27, no. 13, pp. 1702–1714, 2013.

[12] K. Young-Soo and K. Young-Su, "Improve resolution capability via virtual expansion of array," *Electronics Letters*, vol. 35, no. 19, pp. 1596–1597, 1999.

[13] W. R. Hamilton, "On quaternions," *Proceedings of the Royal Irish Academy*, vol. 3, pp. 1–16, 1847.

[14] N. Le Bihan and J. Mars, "Singular value decomposition of quaternion matrices: a new tool for vector-sensor signal processing," *Signal Processing*, vol. 84, no. 7, pp. 1177–1199, 2004.

[15] S. Miron, N. Le Bihan, and J. I. Mars, "Quaternion-MUSIC for vector-sensor array processing," *IEEE Transactions on Signal Processing*, vol. 54, no. 4, pp. 1218–1229, 2006.

[16] N. Le Bihan, S. Miron, and J. I. Mars, "MUSIC algorithm for vector-sensors array using biquaternions," *IEEE Transactions on Signal Processing*, vol. 55, no. 9, pp. 4523–4533, 2007.

[17] X. F. Gong, Z. W. Liu, and Y. G. Xu, "Quad-quaternion MUSIC for DOA estimation using electromagnetic vector sensors," *EURASIP Journal on Advances in Signal Processing*, vol. 2008, 14 pages, 2008.

[18] X. F. Gong, Z. W. Liu, and Y. G. Xu, "Quaternion ESPRIT for direction finding with a polarization sensitive array," in *Proceedings of the International Conference on Signal Processing*, pp. 378–381, Beijing, China, 2008.